Journal of Power Sources 196 (2011) 9346–9351

Contents lists available at ScienceDirect

Journal of Power Sources

journal homepage: www.elsevier.com/locate/jpowsour

Short communication

An advantageous method for methanol oxidation: Design and fabrication of a nanoporous PtRuNi trimetallic electrocatalyst

Wei Wang[a], Rongfang Wang[a,*], Hui Wang[a], Shan Ji[b], Julian Key[b], Xingzhong Li[a], Ziqiang Lei[a,**]

[a] Key Laboratory of Eco-Environment-Related Polymer Materials, Ministry of Education of China, Key Laboratory of Gansu Polymer Materials, College of Chemistry and Chemical Engineering, Northwest Normal University, Lanzhou 730070, China
[b] South African Institute for Advanced Materials Chemistry, University of the Western Cape, Cape Town 7535, South Africa

ARTICLE INFO

Article history:
Received 1 June 2011
Received in revised form 29 June 2011
Accepted 30 June 2011
Available online 8 July 2011

Keywords:
Methanol oxidation
Nanoporous
Trimetallic alloy
Electrocatalysts

ABSTRACT

In this study, an advantageous method of methanol oxidation is developed using a nanoporous structured PtRuNi trimetallic catalyst fabricated by dealloying Ni from a high Ni-content PtRuNi alloy precursor. Transmission electron microscopy (TEM), X-ray diffraction (XRD) and X-ray photoelectron spectroscopy (XPS) are used for catalyst characterization. The nanoporous PtRuNi trimetallic catalyst shows enhanced CO oxidation, higher activity and better stability than solid commercial PtRu/C catalyst. The method developed in this study is well suited to synthesize other high performance, nanoporous-structured, multimetallic electrocatalysts for fuel cells.

1. Introduction

For effective production of electrochemical energy using direct methanol fuel cells (DMFC), stable and efficient electrocatalysts are critically required and fundamental progress in catalyst design is still needed to achieve this goal [1].

The high surface area and unique chemical activity of nanoporous metals have great potential as catalysts [2] and have attracted much attention for methanol oxidation [3–8]. By making nanoparticles nanoporous, their performance can be improved due to their reduced density and increased surface area. At the same time, PtRuM (M = Fe, Co, Ni) trimetallic alloy electrocatalysts, which are more active than the state-of-the-art PtRu electrocatalyst for methanol oxidation, have attracted much attention because the third metal of the alloy can act as a promotion agent [9–15]. However, the combination of a nanoporous/trimetallic system, giving the advantage of nanoporous structure and the superior activity of trimetallic alloy in one catalyst, has received relatively little attention.

Many previous studies show that Ni can modify the behavior of the PtRu/C electrocatalyst and act as an assistant component [16,17]. However, the absence of Ni in the initial catalyst composition also avoids potential contamination and offers better performance and durability [18]. In the present work, a carbon supported nanoporous PtRuNi trimetallic catalyst (denoted as N-PtRuNi/C) is prepared by dealloying Ni from high (80%) Ni-content PtRuNi alloy precursor (denoted as P-PtRuNi/C). The resultant structure retains Ni in its PtRuNi core and is covered by a Ni-depleated nanoporous PtRu shell structure. The high surface area shell and presence of the protected inner Ni-containing core improves the utilization of precious PtRu metals by improving catalytic activity. The results presented here provide considerable insight into the nanoporous multimetallic system and paves the way for its application in fuel cells.

2. Experimental

2.1. Catalyst synthesis

Firstly, H_2PtCl_6 (65.6 mg), $RuCl_3$ (33.8 mg), $NiCl_2{\cdot}6H_2O$ (240.4 mg) and sodium citrate (380.7 mg) were dissolved in water, stirred for 0.5 h. Then the pretreated carbon black (150 mg) (Vulcan XC-72R) was added, stirred and treated in an ultrasonic bath for 0.5 h, afterward, 20 ml hydrazine hydrate was added. The solution was transferred into a Teflon-lined autoclave and heated at 120 °C for 4 h, then centrifuged and washed with deionized water until no chloride anion in the filtrate. The product was dried for 4 h in vacuum at 50 °C and then annealed under flowing N_2 and H_2 at 300 °C for 1 h, respectively. It is denoted as P-PtRuNi/C. Secondly, the P-PtRuNi/C was added to a flask containing H_2SO_4 solution (6 M, 30 ml) and stirred for 24 h. The centrifuged solution

* Corresponding author. Tel.: +86 931 7971533; fax: +86 931 7971533.
** Corresponding author. Tel.: +86 931 7970359; fax: +86 931 7970359.
E-mail addresses: wrf38745779@126.com (R. Wang), leizq@hotmail.com (Z. Lei).

0378-7753/$ – see front matter © 2011 Elsevier B.V. All rights reserved.
doi:10.1016/j.jpowsour.2011.06.101

is green, indicating the Ni dissolved from the P-PtRuNi/C. The product was rinsed several times with ultrapure water and dried in vacuum at 50 °C. The N-PtRuNi/C was obtained. Commercial PtRu/C was used as a reference (Johnson Matthey Company, 30 wt% metal loaded, atom ratio Pt:Ru = 1:1).

2.2. Characterization

Transmission electron microscopy (TEM) measurements were carried out on a JEM-2010 Electron Microscope (Japan) and the energy dispersive X-ray analysis (EDX) technique coupled to TEM. X-ray diffraction (XRD) patterns were recorded on a Rigaku D/Max-2400 (Japan) diffractometer, using Cu Kα radiation operated at 40 kV and 100 mA. X-ray photoelectron spectroscopy (XPS) (Thi-5702 America) is a monochromatic Al Kα X-ray source ($h\nu$ = 29.35 eV).

The electrochemical experiments were performed using an Autolab electrochemical work station (PGSTAT128N, Eco Chemie, Netherlands). A conventional three-electrode cell was used, including an Ag/AgCl (3 M KCl) electrode as the reference, a platinum wire as the counter, and a modified glass carbon (5 mm in diameter) as the working electrode. All potentials presented are quoted with respect to the normal hydrogen electrode (NHE). The working electrode was prepared as follows: 5 mg catalyst was dispersed ultrasonically in 1 mL Nafion/ethanol (0.25% Nafion). 8 μL suspensions were quantitatively transferred to the surface of polished glassy carbon electrode, followed by drying in air.

The CO stripping was characterized in a 0.5 M H_2SO_4 solution. Two consecutive cycles were performed to oxidize pre-adsorbed CO_{ads} on catalysts, and CO pre-adsorption was performed with bubbling carbon monoxide for 30 min. Then the gas was switched to N_2 for 5 min to remove physically adsorbed CO from the gas phase. Electrocatalytic activities for methanol oxidation were measured in the solution of 0.5 M H_2SO_4 + 0.5 M methanol. The solution was purged with high-purity N_2 for at least 30 min to ensure N_2 saturation. All measurements were recorded at a scan rate of 50 mV s^{-1} and rotation speed of 300 rpm after a stable response was established at room temperature.

3. Results and discussion

Recently, low-active-metal-content trimetallic alloys have attracted much attention as electrocatalysts for fuel cells [10,11,14] while less attention has been given to the high-active-metal-content multi-component alloy systems. Using alloy corrosion under appropriate conditions, nanoporous nanostructures with intriguing properties can be made [4,6]. In the present work, we focus on the fabrication of N-PtRuNi trimetallic catalyst. The fabrication procedure is illustrated in Scheme 1. Compared to precious metals (Pt and Ru), the Ni component is much more reactive and is therefore easily leached out in acid. Ni atoms were etched from high (80%) Ni-content PtRuNi alloy precursor to leave a nanoporous structure behind. The remaining nanoporous PtRu shell protects the remaining core Ni atoms from further dissolving thus making them available for promoting the N-PtRuNi catalyst catalytic performance via electronic interaction in the final catalyst. The procedure was as follows: Pt, Ru and Ni were first deposited onto the carbon. Then, the powders were heat-treated at 300 °C to remove the organic moieties and etched in sulfuric acid for 24 h at room temperature. Most of the Ni atoms from the PtRuNi alloy dissolved, while Ru formed the PtRu alloy in the nanoporous surface with some Ni atoms remaining in the nanoporous bulk structure. Therefore, the structure and composition of the N-PtRuNi trimetallic catalyst should be ideal for methanol oxidation.

TEM was used to characterize the surface morphologies of the synthesized carbon supported nanoparticles. As can be seen, P-PtRuNi (Fig. 1A) and N-PtRuNi nanoparticles (Fig. 1B) are dispersed on the carbon support. Both of them show a broader size distribution and are similarly centered around 60 nm (bottom right corner). P-PtRuNi/C nanoparticles are solid (magnified in Fig. 1C), while the N-PtRuNi/C nanoparticles are nanoporous in structure (magnified in Fig. 1D) (black regions are solid metal and bright regions are pores) due to the etching process. The EDX analysis spectra indicated that most of Ni atoms were excavated by dealloying. The EDX composition of P-PtRuNi (Fig. 1E) atom ratio is 1.0:1.0:9.4 (Pt:Ru:Ni), while the N-PtRuNi (Fig. 1F) is 1.0:1.1:2.3. Therefore, dealloying decreased the molar percentage of Ni from 82.45% to 23.25%. Furthermore, the crystalline feature was also confirmed by selected area electron diffraction pattern (Fig. 1A and B top left corner). The P-PtRuNi and N-PtRuNi catalysts adopted a typical face-centered cubic (fcc) polycrystalline structure. However, the crystalline nature of the N-PtRuNi becomes weak compared to P-PtRuNi due to etching process.

XPS was employed to analyze the surface composition in P-PtRuNi/C and N-PtRuNi/C catalysts. As shown in Fig. 2A, peaks can be readily assigned to the binding energies of Pt 4f, Ru 3d, C 1s, Ru 3p and O 1s, respectively [19,20]. The C, O, Pt and Ru are revealed in all the samples. However, the bind energy of Ni 2p is clearly detected only on P-PtRuNi/C. The XPS data of Ni 2p and Pt 4d before and after dealloying are also shown in Fig. 2B and C. The Ni 2p spectrum shows a complicated structure adjacent to the main peaks in Fig. 2B, as reported [21], which is attributed to multi-electron excitation. Taking into account that the escape depth of the photoelectrons is about 3–4 nm [21]. The peaks of Ni 2p disappear almost completely after dealloying, which indicate that exposed Ni on the surface of nanoparticle diluted and that remaining Ni is buried within the nanoporous bulk. Additionally, the Pt $4f_{5/2}$ peaks of the N-PtRuNi shift toward higher binding energy in Fig. 2C, suggesting that the electronic structure of Pt is influenced by the Ru and Ni component

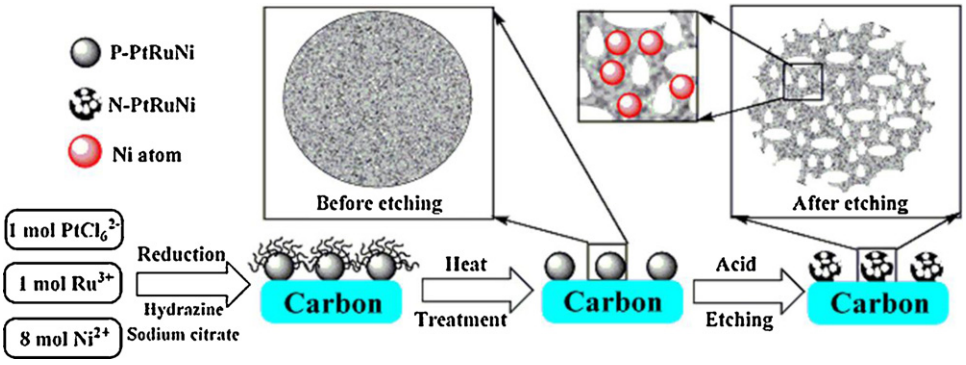

Scheme 1. The designed protocol for N-PtRuNi/C catalyst.

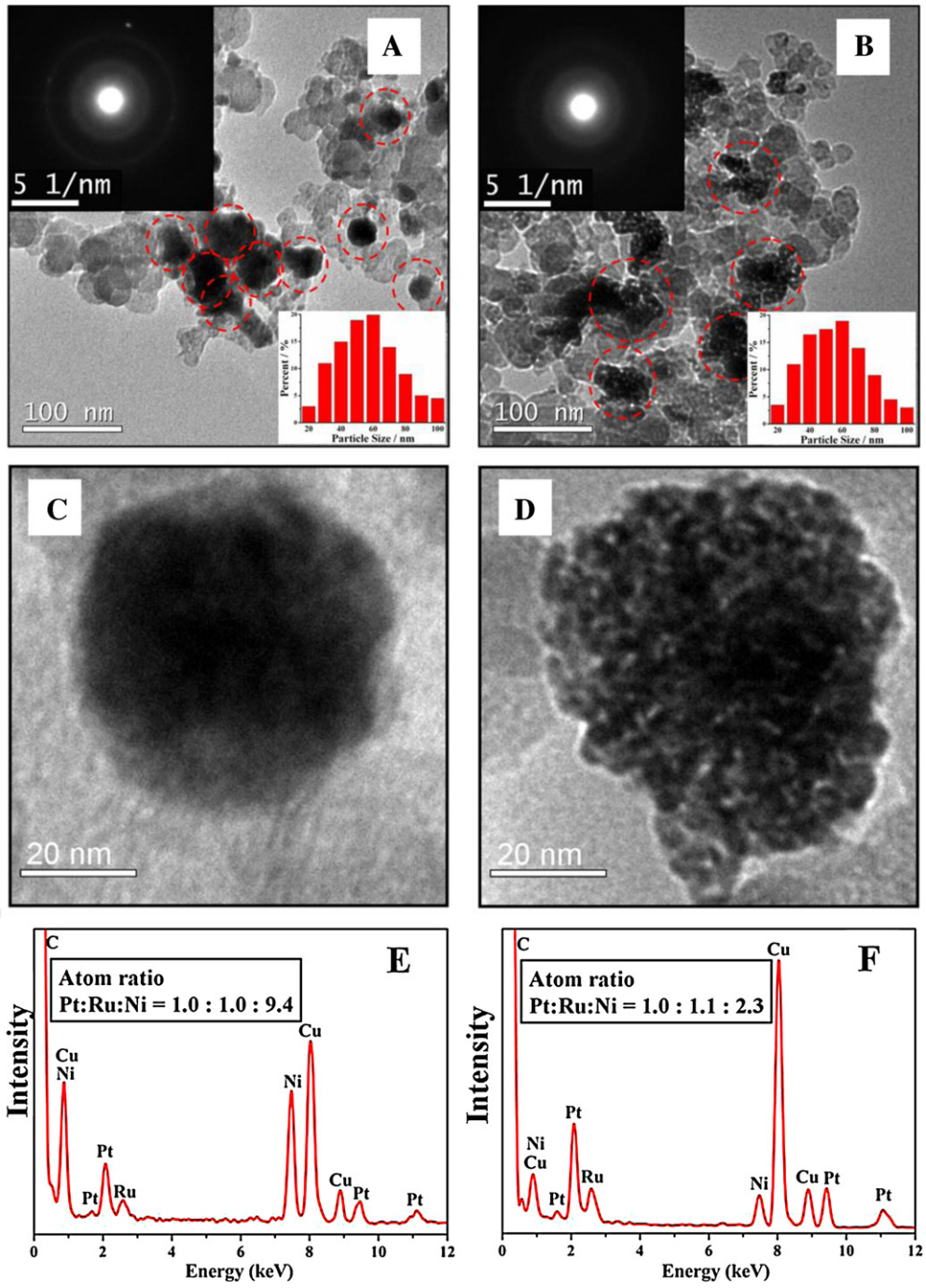

Fig. 1. (A) TEM image of the as-prepared P-PtRuNi/C and (B) N-PtRuNi/C. Inserts in A and B: the corresponding selected area electron diffraction (top left corner) and particle size distribution histograms of catalysts (bottom right corner); (C) the magnification of the as-prepared P-PtRuNi/C and (D) N-PtRuNi/C; (E) EDX of the as-prepared P-PtRuNi/C and (F) N-PtRuNi/C.

in the bulk, which can improve the catalytic activity of Pt in terms of the methanol adsorption/dehydrogenation, activation of water, and CO tolerance [6].

XRD was used to analyze the crystalline structure of N-PtRuNi/C and P-PtRuNi/C. The corresponding XRD patterns are shown in Fig. 2D. The first broad peak at 24.8°, associated with the Vulcan XC-72R support. Other remaining peaks are consistent with a typical face-centered cubic (fcc) structure. It is worthwhile to note that, the (1 1 1) plane of N-PtRuNi/C shifts to lower 2θ value compared to that of P-PtRuNi/C after being dealloyed. Furthermore, the (1 1 1) peak is relatively decreased, which reveals a decrease in the crystallinity of initial P-PtRuNi/C. All the results strongly suggest that the Ni dissolved from the P-PtRuNi/C alloy phase.

CO oxidation (stripping analysis) provides valuable information about the nature of the samples. Both the amount of exposed metal phase and the degree of alloying can be inferred (to a certain extent) from the stripping analysis. The CO stripping is compared in Fig. 3A. A broad peak appears during the first scan and disappears in the subsequent scan, indicating that the adsorbed CO is completely oxidized during the first forward scan. The CO peak of N-PtRuNi/C is located at 0.59 V, which is more negative than that of solid PtRu/C (0.70 V). The onset potential for CO oxidation on N-

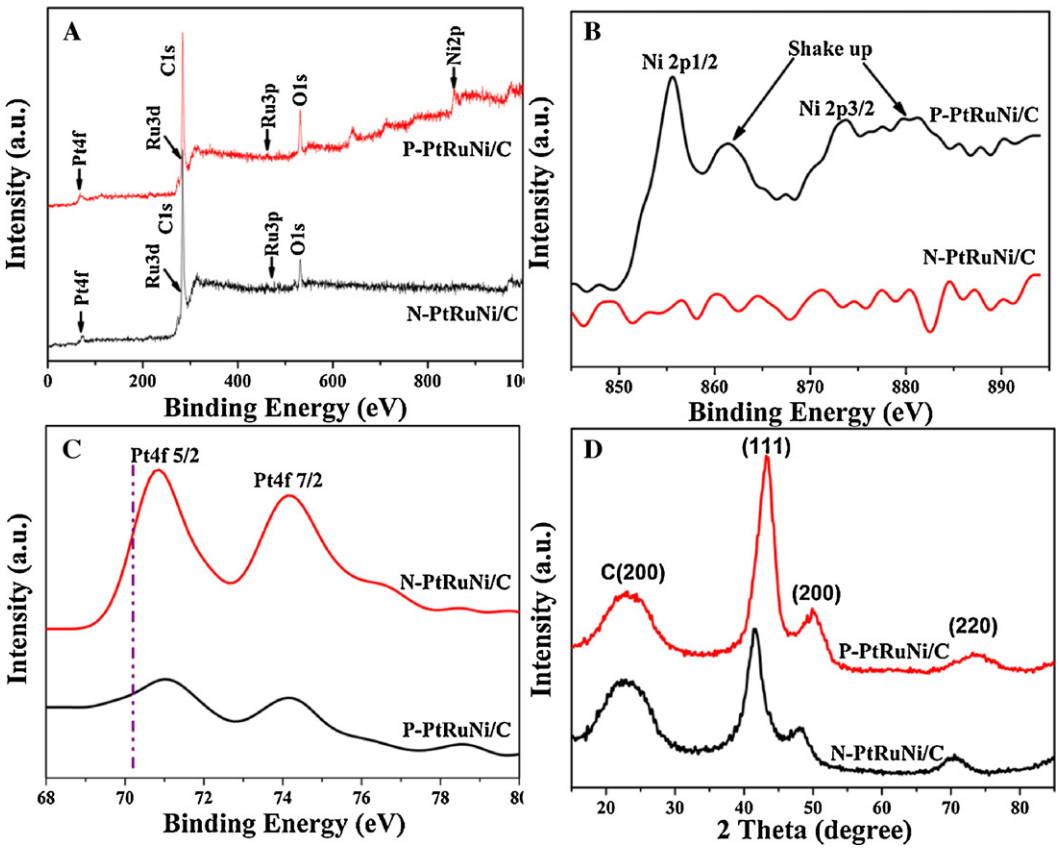

Fig. 2. (A) XPS spectrums of the P-PtRuNi/C and N-PtRuNi/C; (B) Ni 2p XPS spectrums of the P-PtRuNi/C and N-PtRuNi/C; (C) Pt 4f XPS spectrums of the P-PtRuNi/C and N-PtRuNi/C. The dotted line at 71.2 eV is pure Pt $4f_{5/2}$ peak; (D) XRD patterns of P-PtRuNi/C and N-PtRuNi/C.

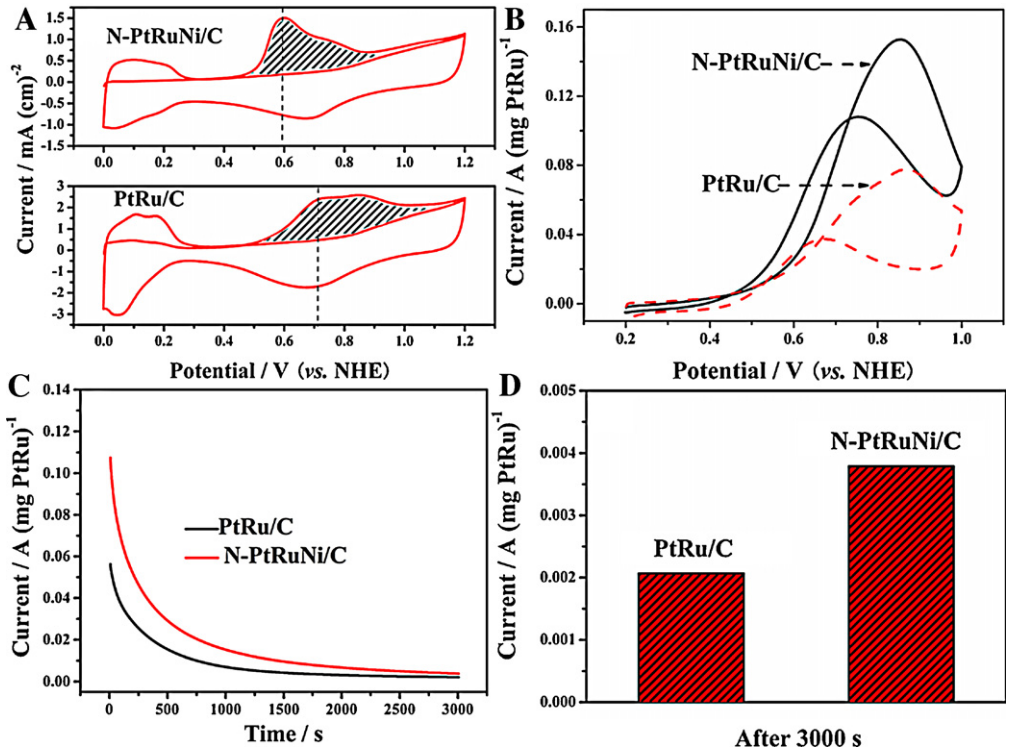

Fig. 3. (A) Cyclic voltammograms for CO stripping on the solid PtRu/C and N-PtRuNi/C catalysts; (B) cyclic voltammograms for methanol oxidation on the solid PtRu/C and N-PtRuNi/C catalysts; (C) chronoamperometric curves of methanol oxidation on the solid PtRu/C and N-PtRuNi/C catalysts for 3000 s. Fixed potential: 0.8 V (*vs.* NHE); (D) chronoamperometry current of methanol oxidation on the solid PtRu/C and N-PtRuNi/C catalysts after 3000 s.

PtRuNi/C (0.40 V) is about 70 mV lower than that on solid PtRu/C (0.47 V). CO is a very stable intermediate resulting from methanol decomposition while simultaneously being a strong poison for the Pt-based electrode and thus reducing its activity [22]. These result indicating a more facile CO removal of the N-PtRuNi/C catalyst, and hence, an improved CO tolerance in practice.

CO electrooxidation is significantly effected by the Ru and Ni [6,16]. There is electron transfer from nickel to platinum in PtNi and probably from ruthenium to platinum in PtRu, in agreement with the electronegativity series for Ni, Ru and Pt [23]. The electron transfer may contribute to the decay of Pt–CO binding energy and enhance the formation of intermediates from methanol electrooxidation. The underlayed Ni and alloyed Ru in the N-PtRuNi/C catalyst would be play an important role for improved CO tolerance.

From the TEM results, N-PtRuNi/C particles are much bigger than those of solid PtRu/C (3.5 nm). However, based on the assumption of 420 mC cm^{-1} surface charges for linearly adsorbed CO [24], the electrochemical surface areas for N-PtRuNi/C and solid PtRu/C catalysts are estimated as 24.4 m^{-2} g^{-1} PtRu and 34.1 m^{-2} g^{-1} PtRu individually, which can be attributed to nanoporous structure having a much higher specific area than a solid one.

Methanol electrooxidation was used as a test reaction to evaluate catalyst activity. As most of the Ni atoms from the P-PtRuNi/C were dissolved and the solid nanoparticle becomes a nanoporous one. The current density was normalized according to the amount of PtRu for methanol electrooxidation, shown in Fig. 3B. The peak currents of the N-PtRuNi/C and PtRu/C catalysts are 0.15227 A mg^{-1} PtRu and 0.07818 A mg^{-1} PtRu, respectively. It is clear that the catalytic activity of the N-PtRuNi/C is 1.9 times than that of PtRu/C. On the basis of the current prices of PtRu, the reduction cost of the N-PtRuNi/C is about 50% of the price of the commercial PtRu/C electrocatalyst price. As to the origin of the enhanced performance of N-PtRuNi catalyst, the underlayed Ni may provide an electronic modification for the topmost metal layer, and the nanoporous structure provides more surface area.

Chronoamperometry was used to further investigate the activity of N-PtRuNi/C for practical application shown in Fig. 3C. As expected, the initial current density for N-PtRuNi/C is much greater than that for the solid commercial PtRu/C, indicating a greater number of active sites available per unit of surface area. Furthermore, methanol oxidation current on N-PtRuNi/C (0.00379 A mg^{-1} PtRu) after 3000 s (Fig. 3D) is higher than that on PtRu/C (0.00207 A mg^{-1} PtRu). This also clearly demonstrates a higher utilization of PtRu metal in the N-PtRuNi/C catalyst.

From a practical point of view, the stability of the material in a DMFC environment is very important. Therefore, the stability was also evaluated by monitoring the loss of current as shown in Fig. 4A. It is obvious that the rate of the degradation of the solid PtRu/C catalyst is higher than that of the N-PtRuNi/C catalyst (78.1% *vs.* 64.1%). Based on the PtRu mass, after 500 cycles the current density of N-PtRuNi/C at peak potentials (0.0927 A mg^{-1} PtRu) is still 1.99 times higher than solid PtRu/C catalyst (0.0465 A mg^{-1} PtRu), further indicating that the present N-PtRuNi/C catalyst has good stability.

Tafel plots of the methanol oxidation on the solid PtRu/C and N-PtRuNi/C catalysts are shown in Fig. 4B. The first fitted Tafel slopes are 101.0 and 103.5 mV dec^{-1} for N-PtRuNi/C and solid PtRu/C at low potentials (<0.65 V *vs.* NHE), respectively. While the second Tafel slopes are 202.3 and 220.3 mV dec^{-1} at high potentials (0.65–0.75 V, *vs.* NHE). The second slopes are almost double the first ones, indicating a possible change of reaction mechanism or at least a transformation of rate-determining step at different potentials range [25].

In the first region at low potentials, the fitted Tafel slopes of solid PtRu/C and N-PtRuNi/C catalysts are very close to the theoretical value (118 mV dec^{-1}) [26] and that of previously reported data (110–140 mV dec^{-1}) [27,28]. This indicates that the unit reaction involving the splitting of the first C–H bond of methanol molecules with the first electron transfer is the rate-determining step at low potentials [26]. With increasing potential, the adsorbed CO-like residues are gradually oxidized and thus the active sites on platinum are cleaned up for the subsequent methanol dehydrogenation reaction. The change in the second Tafel slopes may be attributed to the insufficient compensation of methanol oxidation for the rapid oxidation reaction on the electrode surface, and mass transfer of methanol at high potential is hypothesized to be the rate-determining step [29].

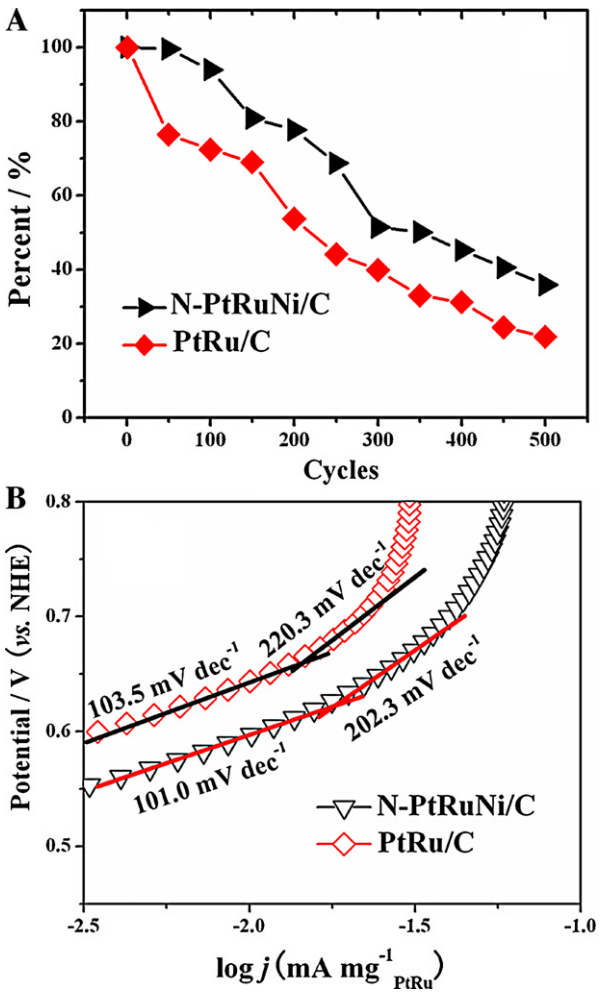

Fig. 4. (A) Decreases of peak currents of solid PtRu/C and N-PtRuNi/C catalysts on potential cycling in 0.5 mol L^{-1} CH_3OH + 0.5 mol L^{-1} H_2SO_4 between 0 and 0.8 V; (B) Tafel plots of methanol oxidation on solid PtRu/C and N-PtRuNi/C catalysts in 0.5 mol L^{-1} CH_3OH + 0.5 mol L^{-1} H_2SO_4 solution under N_2 atmosphere. Scan rate: 5 mV s^{-1}.

As can be seen from the above results, the performance of the N-PtRuNi/C catalyst was better than that of the solid PtRu/C catalyst for methanol electrooxidation. Meanwhile, the N-PtRuNi/C and solid PtRu/C catalysts had the same contents of Pt and Ru. Both the nature of underlayer Ni and the nanoporous structure may play a marked role in the performance and promotion of methanol electrooxidation. Therefore, the enhanced electrocatalytic activity of the N-PtRuNi/C electrode may result from the Ni element. The Ni could plays two important roles: (i) Acid leaching of Ni forms a porous structure, which provides more specific area for methanol electrooxidation; (ii) as in the PtRuNi catalyst [16–18], the remaining underlayed Ni modifies the behavior of PtRu/C electrocatalyst

and acts as an assistant component for enhanced CO oxidation and methanol oxidation.

4. Conclusions

Carbon supported N-PtRuNi catalyst, prepared by dealloying Ni from high Ni-content P-PtRuNi alloy, showed enhanced CO oxidation, higher activity and better stability than that of solid PtRu/C catalyst for methanol oxidation. Because the trimetallic alloy nanoporous nanostructure has relatively lower densities and higher surface areas than solid counterparts, and thus improved performance, this strategy is well suited to synthesize other excellent electrocatalysts for fuel cells. Considering the advantages of higher utilization of PtRu and the enhanced electrocatalytic activity and stability, the N-PtRuNi/C is a promising electrocatalyst for use in DMFC.

Acknowledgments

The Key Project of Ministry of Education Foundation of China (209129), and the Scientific and Technical Innovation Project of Northwest Normal University (NWNU-kjcxgc-03-63) are financially supporting this work.

References

[1] P. Strasser, S. Koh, T. Anniyev, J. Greeley, K. More, C. Yu, Z. Liu, S. Kaya, D. Nordlund, H. Ogasawara, M.F. Toney, A. Nilsson, Nat. Chem. 2 (2010) 454–460.
[2] M. Klein, B.W. Jacobs, M.D. Ong, S.J. Fares, D.B. Robinson, V. Stavila, G.J. Wagner, I. Arslan, J. Am. Chem. Soc. 13 (2011) 9144–9147.
[3] X. Ge, X. Yan, R. Wang, F. Tian, Y. Ding, J. Phys. Chem. C 113 (2009) 7379–7384.
[4] K. Koczkur, Q. Yi, A. Chen, Adv. Mater. 19 (2007) 2648–2652.
[5] R. Wang, C. Wang, W.B. Cai, Y. Ding, Adv. Mater. 22 (2010) 1845–1848.
[6] C. Xu, L. Wang, X. Mu, Y. Ding, Langmuir 26 (2010) 7437–7443.
[7] J. Snyder, P. Asanithi, A.B. Dalton, J. Erlebacher, Adv. Mater. 20 (2008) 4883–4886.
[8] C. Xu, H. Qiu, Y. Liu, Electrochem. Commun. doi:10.1016/j.elecom.2011.04.007.
[9] Z.B. Wang, G.P. Yin, Y.Y. Shao, B.Q. Yang, P.F. Shi, P.X. Feng, J. Power Sources 165 (2007) 9–15.
[10] T. Huang, X. Wang, J. Zhuang, W.B. Cai, A. Yu, Electrochem. Solid-State Lett. 127 (2009) B112–B115.
[11] M.K. Jeon, J.Y. Won, K.R. Lee, S.I. Woo, Electrochem. Commun. 9 (2007) 2163–2166.
[12] V.A. Ribeiro, O.V. Correa, A.O. Neto, M. Linardi, E.V. Spinacé, Appl. Catal. A: Gen. 372 (2010) 162–166.
[13] D.K. Kang, C.S. Noh, N.H. Kim, S.H. Cho, J.M. Sohn, T.J. Kim, Y.K. Park, J. Ind. Eng. Chem. 16 (2010) 385–389.
[14] T. Huang, J. Liu, R. Li, W. Cai, A. Yu, Electrochem. Commun. 11 (2009) 643–646.
[15] J. Liu, J. Cao, Q. Huang, X. Li, Z. Zou, H. Yang, J. Power Sources 175 (2008) 159–165.
[16] M.V. Martinez-Huerta, S. Rojas, J.L.G. Fuente, P. Terreros, M.A. Pena, J.L.G. Fierro, Appl. Catal. B: Environ. 69 (2006) 75–84.
[17] B. Moreno, E. Chinarro, J.C. Pérez, J.R. Jurado, Appl. Catal. B: Environ. 76 (2007) 368–374.
[18] J. Zhao, A. Manthiram, Appl. Catal. B: Environ. 101 (2011) 660–668.
[19] H.S. Qian, Chem. Mater. 18 (2006) 2102–2108.
[20] F. Liu, J.Y. Lee, W.J. Zhou, Small 2 (2006) 121–128.
[21] K.W. Park, J.H. Choi, B.K. Kwon, S.A. Lee, Y.E. Sung, H.Y. Ha, S.A. Hong, H.H. Kim, A. Wieckowski, J. Phys. Chem. B 106 (2002) 1869–1877.
[22] P. Ferrin, M. Mavrikakis, J. Am. Chem. Soc. 131 (2009) 14381–14389.
[23] Z.B. Wang, G.P. Yin, J. Zhang, Y.C. Sun, P.F. Shi, Electrochim. Acta 51 (2006) 5691–5697.
[24] X.H. Jian, D.S. Tsai, W.H. Chung, Y.S. Huang, F.J. Liu, J. Mater. Chem. 19 (2009) 1601–1607.
[25] J. Zhu, F. Cheng, Z. Tao, J. Chen, J. Phys. Chem. C 112 (2008) 6337–6345.
[26] G. Wu, L. Li, B.Q. Xu, Electrochim. Acta 50 (2004) 1–10.
[27] S.L. Gojkovic, T.R. Vidakovic, Electrochim. Acta 47 (2001) 633–642.
[28] S.L. Gojkovic, T.R. Vidakovic, D.R. Durovic, Electrochim. Acta 48 (2003) 3607–3614.
[29] Y.J. Kim, W.H. Hong, S.I. Woo, H.K. Lee, J. Power Sources 159 (2006) 491–500.